Available online at www.sciencedirect.com
ScienceDirect
Journal of Photochemistry and Photobiology A: Chemistry 184 (2006) 125–134
Journal of Photochemistry and Photobiology A:Chemistry
www.elsevier.com/locate/jphotochem

Adsorption and photocatalytic degradation of diisopropyl fluorophosphate and dimethyl methylphosphonate over dry and wet rutile TiO_2

A. Kiselev [a,b], A. Mattson [a], M. Andersson [c], A.E.C. Palmqvist [c], L. Österlund [a,*]

[a] *Department of Environment and Protection, FOI NBC Defence, Cementv. 20, SE-901 82 Umeå, Sweden*
[b] *Department of Inorganic Chemistry, Umeå University, SE-901 87 Umeå, Sweden*
[c] *Applied Surface Chemistry, Department of Chemical and Biological Engineering, Chalmers University of Technology, SE-412 96 Göteborg, Sweden*

Received 23 February 2006; received in revised form 30 March 2006; accepted 3 April 2006
Available online 18 April 2006

Abstract

Nanosized, crystalline rutile TiO_2 was synthesized at room temperature using a microemulsion-mediated system followed by hydrothermal treatment. The formed rutile had a specific surface area of about 40 $m^2\,g^{-1}$ and the rutile crystals had dimensions of about 10 nm × 150 nm, which aggregated into 200–1000 nm sized bundles. The adsorption and photocatalytic degradation of diisopropyl fluorophosphate (DFP) and dimethyl methylphosphonate (DMMP) over these rutile TiO_2 nanoparticles in dry and wet synthetic air was investigated by in situ diffuse reflectance Fourier transform infrared (DRIFT) spectroscopy during simulated solar light illumination. The methyl and isopropyl groups do not dissociate upon adsorption on either dry or humidified rutile nanoparticles. The F atom in DFP is, however, easily hydrolyzed and is readily dissociated upon interaction with hydroxyls on the TiO_2 surfaces and leads to a destabilization of the DFP molecule. The initial solar light induced photodegradation rate for DFP and DMMP is 5.9×10^{-4} and 1.0×10^{-4} s^{-1} in dry conditions and 8.1×10^{-4} and 0.7×10^{-4} s^{-1} in wet conditions (corresponding to 2–3 monolayers (ML) water coverage), respectively. The main intermediate partial oxidation surface products are found to be surface bound formate-carboxylate-carbonate (R–COO^-) and phosphate (R–POO^-) species. Among them η^1-coordinated acetone and μ-formate, bicarbonate, and bidentate R–POO^- moieties are detected. These surface species accumulate on the surface during the entire illumination period (60 min), and lead to a decreased total oxidation rate. Controlled humidification of the rutile surface leads to a reduction of the concentration of R–COO^- intermediates, while at the same time maintaining approximately the same rate of DFP and DMMP photooxidation. The latter is due to blocking of Ti surface cation sites, which prevents the formation of strongly bonded surface compounds, in particular μ-coordinated R–COO^- and R–POO^- species. The findings show that, it is possible to optimize the sustained photocatalytic degradation of organic phosphorous compounds by controlled humidification of the reaction gas.

Keywords: Photocatalysis; TiO_2; Rutile; Nanoparticles; Organic phosphorous compounds; Dimethyl methylphosphonate; Diisopropyl fluorophosphate

1. Introduction

Photocatalysis denotes the acceleration of a photoreaction by the action of a catalyst [1–4]. In the present context we use a more narrow description, i.e. the oxidative degradation of organic pollutants by an UV irradiated semiconductor, notably TiO_2, which is by far the most commonly used photocatalyst. A wide array of organic substances containing O, N, S, P, and halogen atoms can be oxidized by this photochemical method. Hence, this route provides a convenient oxidative degradation method requiring no unstable and potentially dangerous chemical oxidants. Photocatalysis is therefore, an attractive environmentally benign method for decontamination of organic phosphorous impurities, including warfare agents and pesticides. There is today a general understanding of the photocatalytic action of TiO_2, albeit fundamental questions regarding, e.g. interfacial charge transfer mechanisms and deactivation still exist [1–3]. Briefly, light with energy larger than the optical band gap of TiO_2 (>3.0 eV for rutile) creates an electron hole pair, which is trapped via interfacial electron transfer by appropriate redox-active adsorbates. On a humidified surface or in the aqueous phase, oxidation of adsorbed water or OH^- by the hole produces hydroxyl radicals ($^{\bullet}OH$), while reduction of O_2 produces O^{2-} or O^- radicals, both of which are extremely powerful and indiscriminating oxidants

* Corresponding author. Tel.: +46 90 106900; fax: +46 90 106802.
E-mail address: lars.osterlund@foi.se (L. Österlund).

1010-6030/$ – see front matter © 2006 Elsevier B.V. All rights reserved.
doi:10.1016/j.jphotochem.2006.04.005

that attack pollutants at the surface resulting in their oxidative degradation. The photocatalytic conversion rate (decomposed molecules per active site per second) depends on several aspects: surface structure (including type of crystal facet of the photocatalyst), surface area, particle size, amount of OH groups present on surface, etc. The role of surface hydroxyl groups are manifold: they act both as hole scavenger and source of radical formation [1,5,6], while at the same time they can block surface sites for direct coordination of pollutants to the surface. The role of water in photocatalysis is not resolved in the literature. Some authors report that the presence of water in the atmosphere inhibits the photocatalytic degradation of organic compounds [7,8]. Other authors demonstrate that water enhance photocatalytic oxidation of organic molecules [9,10]. Recently we have demonstrated that it is possible to tune the relative humidity of the reaction gas and photocatalyst temperature to optimize the sustained photocatalytic conversion of propane over anatase TiO_2 [11].

In this paper, we present a comparative study of the photocatalytic oxidation of simile chemical warfare agents, diisopropyl fluorophosphate (DFP) and dimethyl methylphosphonate (DMMP), over rutile nanoparticles prepared by hydrothermal treatments of microemulsions in dry and humid environment. We use rutile for two reasons: (i) it is known that the exposed crystal facet of rutile particles are dominated by (1 1 0) facets [12,13], (ii) large rutile particles are readily synthesized due to their thermodynamical stability, and oxidation of organics leads to the formation of stable bridging bidentate formate-carboxylate-carbonate ($R–COO^-$) species on TiO_2, which are particularly pronounced on the rutile (1 1 0) facets [12,14]. Thus, rutile is anticipated to give a more narrow distribution of surface species than on, e.g. anatase nanoparticles [13]. We use this property to monitor the concentration of intermediates at varying reaction conditions using in situ diffuse reflectance Fourier transform infrared (DRIFT) spectroscopy, which is the superior technique to follow reaction intermediates at solid surface at atmospheric pressures [15]. We identify key intermediates that form upon solar light illumination and show that humidification of the surface leads to significantly less coordinatively bonded carboxylate and phosphorous species at the surface. These findings suggest that it is possible to reduce the influence of unwanted surface intermediates, which previously are known to accumulate and limit the total oxidation on TiO_2 in the case of hydrocarbons in general [15] and acetone, propane, DFP and DMMP oxidation in particular [14,16–18].

2. Experimental

Rutile nanoparticles were synthesized using a reversed microemulsion system, which has been described earlier [19,20]. It consisted of TritonX-100 (*tert*-octylphenoxypolyethoxyethanol) as surfactant, 1-hexanol (98% GC) as cosurfactant, and cyclohexane (99%) as the continuous oil. Titanium (IV) butoxide (97%) was used as titania precursor and pre-mixed for 5 min in 5 M nitric acid, which constituted the aqueous phase. The composition of the microemulsion is shown in Table 1 and was prepared at room temperature. The titanium containing microemulsion was put into a stainless steel autoclave and hydrothermally treated at 120 °C for 12 h. The formed titania was found as a precipitate at the bottom of the autoclave and was washed with ethanol and centrifuged repeatedly for five times. All chemicals used for the material synthesis were purchased from Aldrich and used as received.

Table 1
The composition of the microemulsion used for preparing the rutile nanoparticles

	Component	Volume (ml)
Titania precursor	Tetrabutyl titanate	0.85
Aqueous component	HNO_3 (5 M)	2
Surfactant	TritonX-100	2.5
Cosurfactant	*n*-Hexanol	1.5
Oil component	Cyclohexane	4

The synthesized particles were characterized by N_2-adsorption, X-ray diffraction (XRD) and transmission electron microscopy (TEM). Nitrogen adsorption and desorption isotherms were collected at 77 K using a Micromeretic TriStar instrument. Before the physisorption measurements the samples were exposed to vacuum treatment for 12 h at 120 °C to remove remaining moisture. The specific surface area was obtained using the BET method. XRD patterns were obtained on a Siemens D5000 X-ray diffractometer equipped with a Cu Kα radiation source ($\lambda = 1.54$ Å). Scans were collected on washed and dried powders in the 2θ range of 20–60°. TEM was performed on a JEOL 1200 EX II microscope equipped with a Wolfram filament operated at 120 kV accelerating voltage. The sample powders used for TEM were ground in an agate mortar, dispersed in ethanol and placed on a holey carbon grid, and finally dried in open air for 2 h, prior to TEM investigation.

Solar light induced degradation experiments were done in a temperature controlled reaction cell situated in a Bruker IFS-66v/S FTIR spectrometer equipped with a broad band HgCdTe detector and connected to a home-built gas generation system. In situ diffuse reflectance Fourier transform infrared (DRIFT) spectra of powder samples of TiO_2 were acquired during adsorption and decomposition of DFP and DMMP. In each measurement series 50 mg TiO_2 powder was added to the reaction cell. The DRIFT spectra were collected in diffuse reflectance mode with 2 cm^{-1} resolution and 32 scans were co-added as a function of time with a time separation of 30 s between each measurement. The background was collected in a 100 ml/min feed of 20% O_2 in N_2 (AGA research grade) on a clean TiO_2 sample unless otherwise stated. Before each measurement the sample was cleaned in a feed of 20% O_2 in N_2 at 673 K for 15 min and cooled in the same feed to 293 K, where all measurements were performed. The resulting surface is referred to as dry rutile, even though the surface is partially hydroxylated as evidenced by the DRIFT spectra. The wet rutile was prepared by flowing humidified synthetic air over the sample. Humidification of the reaction gas was achieved by passing the synthetic air through a temperature controlled water bath (5 ± 0.2 °C). The water concentration was independently checked by measuring the relative humidity and calculating the relative water concentration. A relative humidity of 7% was employed in the present study. The water uptake on TiO_2 was monitored spectrometrically by following

the water DRIFT absorption bands. The saturation water coverage thus obtained was used to set the experimental time scale for the gas dosing, and is estimated to be 2–3 monolayers (ML) of water [11]. A calibrated amount of DFP (11 μg min^{-1}; Koch-Light Labs, purity 84 ± 5%) and DMMP (10 μg min^{-1}; Aldrich, purity 97%) was added to the feed by passing it through a closed loop gas generator containing a diffusion tube set up in contact with a DFP or DMMP liquid reservoir, as described elsewhere [16,21]. The main impurities were identified by NMR in separate experiments as DFP and DMMP decomposition products containing –F, $–CH(CH_3)_2$ (DFP) and $–O–CH_3$ (DMMP) fragments yielding HF, 2-propanol (DFP) and methanol (DMMP) [16].

X-ray photoelectron spectroscopy (XPS) measurements were made with a Kratos Axis Ultra electron spectrometer using a monochromatic Al Kα source operated at 225 W and a low-energy electron gun for charge compensation. High-resolution scans were acquired using pass energy of 20 eV and an energy resolution of 0.1 eV. The hybrid lens mode was used in all measurements. The binding energy scale was calibrated against the C 1s line of aliphatic carbon, set at 285.0 eV. Atomic concentrations (at.%) were derived from photoelectron peak areas using Shirley or linear background subtraction, the instrumental sensitivity factors and a transmission function appropriate to the acquisition conditions.

Solar light illumination was simulated by a 200 W Xe arc lamp source with a focusing lens assembly combined with AM1.5 filters as described elsewhere [21]. A fused silica fiber optics bundle was used to direct the UV light into the reaction cell. The total photon power was measured with a thermopile detector. In the present work a total power of 166 mW cm^{-2} was employed, which results in approximately 23 mW cm^{-2} at λ < 411 nm (corresponding to the band gap energy of rutile).

3. Results and discussions

3.1. Photocatalyst characterization

In Fig. 1A the XRD pattern of the formed titania is shown. The positions of the Bragg peaks correspond well with that of pure rutile, and by applying the Scherrer equation, the size of the crystals were calculated from the full width at half maximum (FWHM) of the (1 1 0) diffraction peak. In Fig. 1B a TEM micrograph of the TiO_2 nanoparticles is shown and displays the typical rod-shaped morphology of rutile particles exposing (1 1 0) facets [12,19]. The rutile particles have sizes of about 10 nm × 150 nm (compared to a mean 9 nm as determined from XRD) and exist as agglomerates having a diameter of 200–1000 nm. The inset in Fig. 1B shows a selected area electron diffractogram of the sample and it confirms the XRD data and shows that the sample contains pure rutile particles. The specific surface area (BET) of the sample was measured before and after the photocatalytic experiment and there was a pronounced decrease from 40 to 12 m^2 g^{-1} in the case of DFP photooxidation. This indicates that the rutile particles grow in size during the photocatalytic reaction. We will not elaborate further on this ageing phenomenon in the present paper. We merely note that similar observations, although not so dramatic, have previously been reported for anatase TiO_2 nanoparticles [7,11].

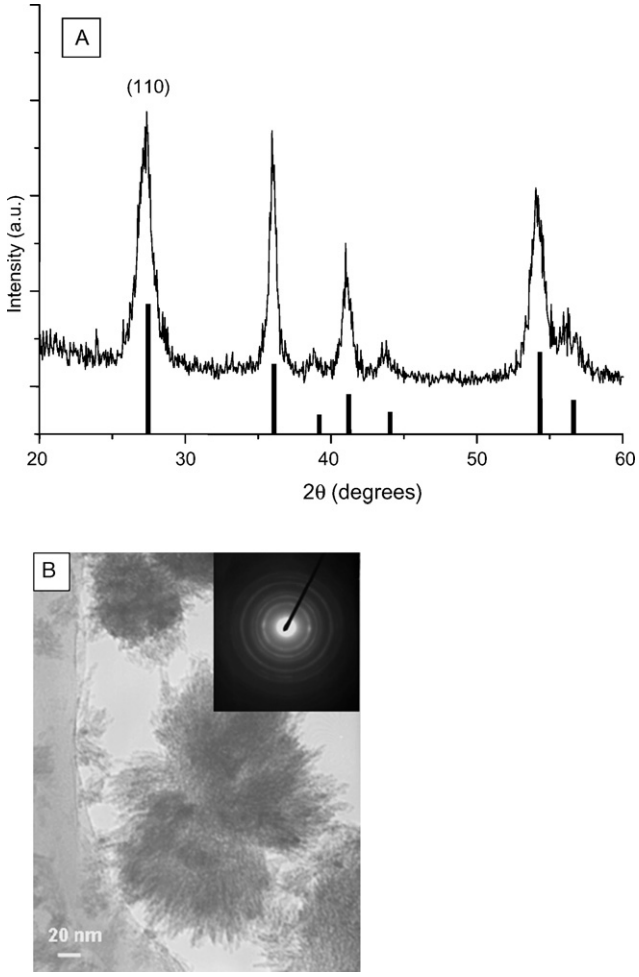

Fig. 1. (A) XRD diffractogram of the formed titania together with the positions of the Bragg peaks corresponding to rutile; (B) TEM micrograph of the formed rutile together with a selected area electron diffractogram (inset).

3.2. Adsorption of DFP and DMMP

Figs. 2 and 3 show DRIFT spectra obtained for rutile TiO_2 after exposure to DFP and DMMP for a total of 20 min. In accordance with previous reports [16,17,22,23], we can propose the following interpretation of the DRIFT spectra. Adsorption of DFP on dry rutile (Fig. 2A) is characterized by the ν(C–O–(P)) absorption band at 1046 cm^{-1} and the ν(P=O) bands at 1250 and 1280 cm^{-1}, as typically observed for organophosphorus compounds [23]. It is known, that the adsorption takes place on acid surface sites. A dry rutile surface has two main types of active sites for –P=O coordination: exposed cation Ti surface sites (I) and Ti–O–H sites (II). In accordance with Sokrates [23] the position of the ν(P=O) frequency strongly depends on the electronegativity of attached groups. Adsorption of DFP on type I sites leads to a ν(P=O) mode at a higher frequency (1280 cm^{-1}), compared to hydrogen bonding, which takes place if DFP molecule adsorbs on type II sites. Hydrogen bonding of DFP leads to a lower frequency of the ν(P=O) vibration

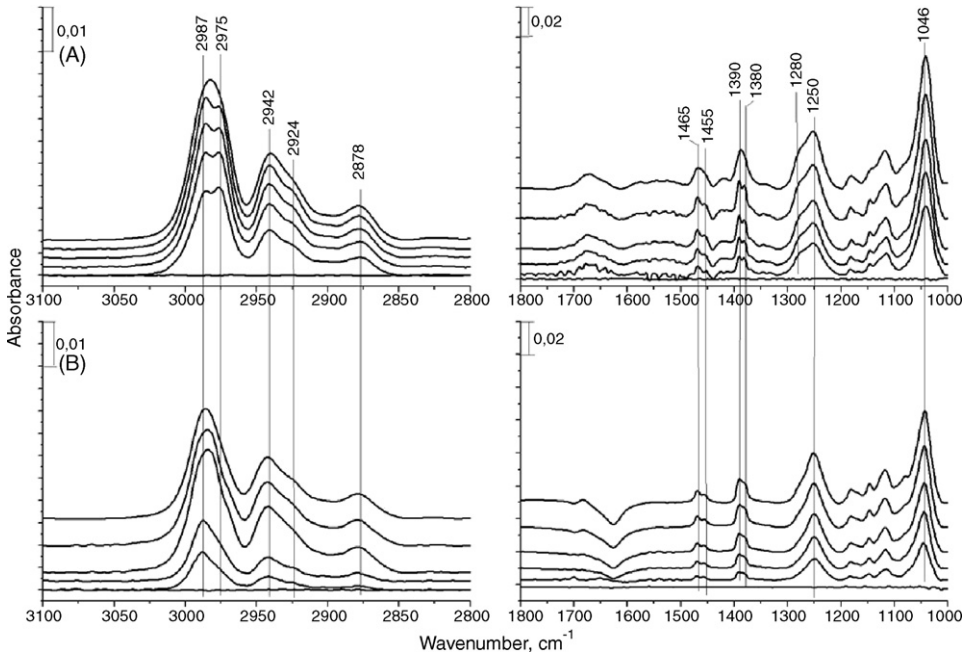

Fig. 2. Diffuse reflectance FTIR spectra collected during 20 min of DFP exposure for dry (A) and humidified (B) rutile TiO_2, respectively. Each of the displayed spectra is separated by 4 min (top to bottom).

(1250 cm^{-1}) and concomitant reduction of the vibrational bands at 3673, 3655 and 3404 cm^{-1} (not shown), which correspond to different types of Ti–OH groups [24]. On a humidified surface (2–3 ML), water molecules block all type I sites. As a result, only hydrogen bonded ν(P=O) band at 1250 cm^{-1} is observed in spectra recorded in wet environment (Fig. 2B). The set of peaks between 1200 and 1100 cm^{-1} should be assigned to the O–$CH(CH_3)_2$ rocking modes [22]. The peaks at 1380, 1390 and 1455, 1465 cm^{-1} correspond to the $\delta_s(CH_3)$ and $\delta_{as}(CH_3)$ modes of *i*Pr groups in DFP and 2-propanol, respectively. 2-propanol is the main contamination in DFP as found by NMR. This molecule is readily oxidized to acetone (see below), with its characteristic ν(C=O) absorption band at 1685 cm^{-1}.

The DRIFT spectra obtained for DMMP on dry rutile (Fig. 3A) are distinct from DFP in several ways. The broad bands in 1250–1100 cm^{-1} region consist of two peaks: ν(P=O)

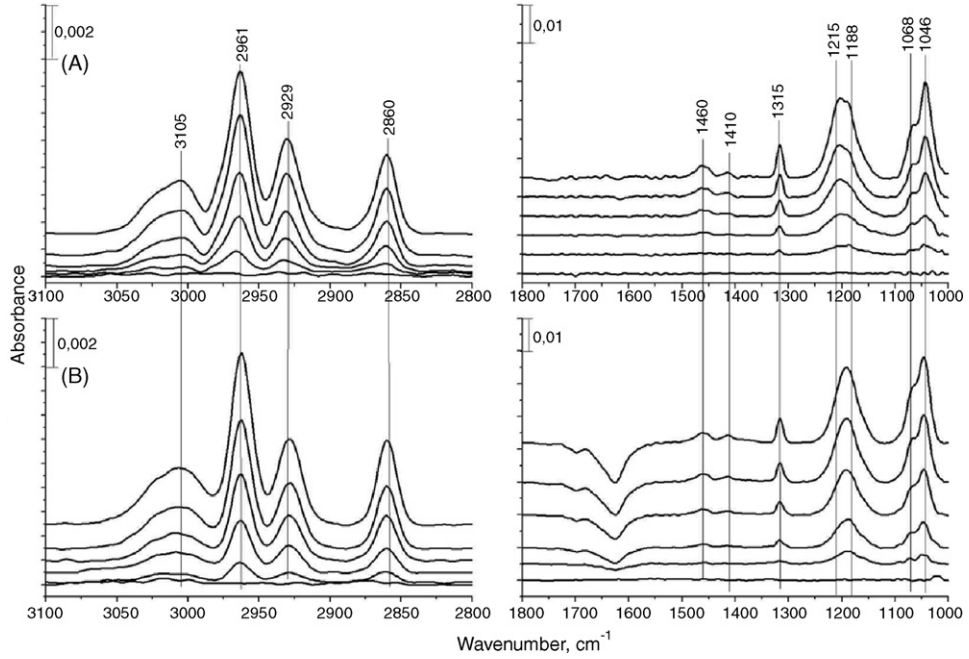

Fig. 3. Diffuse reflectance FTIR spectra collected during 20 min of DMMP exposure for dry (A) and humidified (B) rutile TiO_2, respectively. Each of the displayed spectra is separated by 4 min (top to bottom).

Table 2
Vibrational mode assignments and vibrational frequencies of adsorbed DFP and DMMP on dry rutile

Mode assignments	DFP, $\bar{\nu}$ (cm^{-1})	DMMP, $\bar{\nu}$ (cm^{-1})
$\nu_a(CH_3P)$	–	3015
$\nu_a(CH_3O)$	–	2961
$\nu_s(CH_3P)$	–	2929
$\nu_s(CH_3O)$	–	2860
$\nu_a(CH_3C)$	2987	–
$\nu_s(CH_3C)$	2942	–
ν(CH)	2878	–
$\delta_{as}(CH_3C)$	1465	–
$\delta_s(CH_3C)$	1390	–
$\delta_{as}(CH_3O)$	–	1460
$\delta_a(CH_3P)$	–	1411
$\delta_s(CH_3P)$	–	1315
ν(P=O)	1250	1215
$\rho(CH_3P)$	–	1188
ν_a(C–O)	–	1068
ν_s(C–O)	1046	1046

with maximum at 1215 cm^{-1} and ρ(P–CH_3) with maximum at 1190 cm^{-1}. The sharp peak observed at 1315 cm^{-1} is assigned to the δ_a(P–CH_3) mode. In contrast to DFP, both symmetric (1046 cm^{-1}) and asymmetric (1068 cm^{-1}) modes of ν(C–O–(P)) vibration appear as very distinct peaks in the DMMP spectra. This is probably due to the fact that in DMMP the P–CH_3 group remains non-dissociated upon adsorption on rutile, while for DFP the F atom is abstracted from the P atom, which leads to a destabilization of DFP. The latter affects the isopropyl groups either by association effects (with adjacent adsorbed molecules) and/or charge redistribution, e.g. by coordination with surface sites, which both are expected to result in modifications of the DFP ν(C–O–(P)) vibration [23]. The vibrational mode assignments for the DFP/rutile and DMMP/rutile systems are presented in Table 2. As discussed above, it is well known that the position of the band due to the ν(P=O) stretching vibration is insensitive to the type of compound in which the group occurs, but sensitive to electronegative elements directly bonded to it as well as association effects. The ν(P=O) peak is typically shifted to lower frequency when the P=O group is η^1-coordinated to a cation site, which is the case for DFP and DMMP is adsorbed on TiO_2 [16,17,22,23]. Similarly, electronegative groups such as halogens directly bonded to the phosphorus atom (fluorine atom in case of DFP) partially withdraw electron density from the phosphorous atom thus competing with the oxygen, which otherwise would have a tendency to form P^+–O^-. This explains why the ν(P=O) bond in DFP has a higher frequency than in DMMP as seen in Figs. 2 and 3. In the corresponding liquid spectra (not shown) the ν(P=O) frequency in DFP (~1290 cm^{-1}) is also significantly higher than in DMMP (~1245 cm^{-1}).

The integral intensity of the ν(C–O–(P)) vibration was extracted as a function of gas exposure time and normalized to integral intensity of the ν(CH) vibrations (between 2800 and 3100 cm^{-1}) obtained after 20 min of DFP and DMMP dosing, respectively. The intensity of the ν(C–O–(P)) thus obtained is shown in Fig. 4. The Elovich equation [25] has previously been

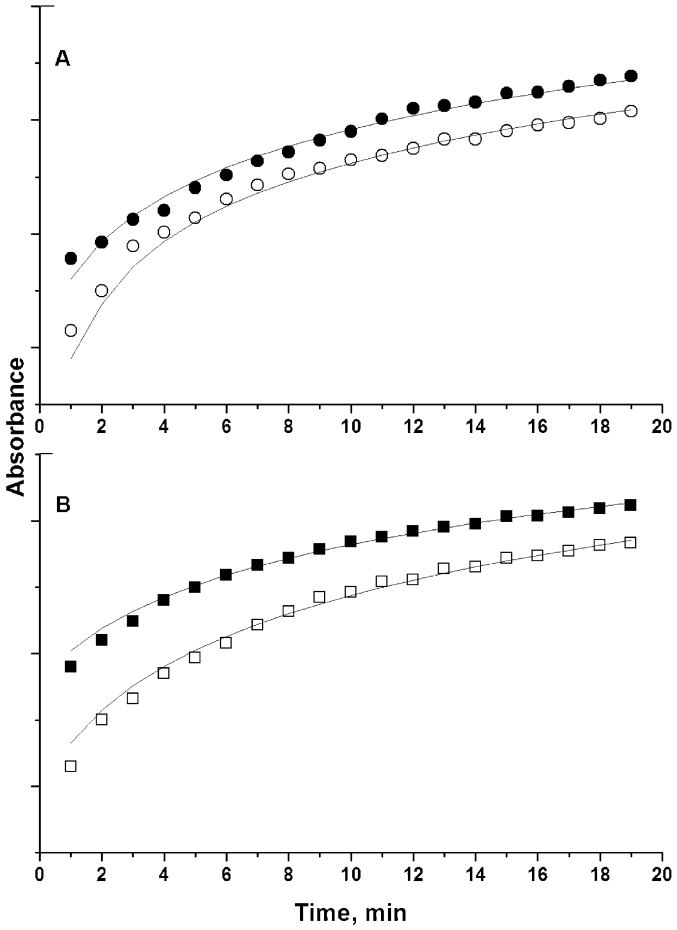

Fig. 4. The integrated intensity of the ν(C–O–(P)) mode in DFP adsorbed on a dry (■) and wet (□) rutile surface, and in DMMP adsorbed on a dry (●) and wet (○) rutile surface. The solid lines show the results of a least square fitting to the Elovich equation.

reported to describe the adsorption of organic phosphorous compounds well [26]. A least-square fit of the experimental data to the Elovich equation is shown as solid lines in Fig. 4, which are seen to describe the data well. This is in perfect agreement with the DRIFT data and provides further support that the methyl and isopropyl groups of the DFP and DMMP molecules do not dissociate during adsorption on rutile (wet or dry).

3.3. Photocatalytic decomposition of DFP and DMMP

Figs. 5 and 6 show DRIFT spectra obtained during 20 min of solar light illumination of rutile samples with preadsorbed DFP and DMMP on a dry (A) and wet (B) surface, respectively. The vertical dashed lines indicate the new peaks, which appear during illumination as the peaks associated with the methyl and isopropyl groups in DMMP and DFP decrease. The data show that isopropyl groups in case of DFP and methyl groups in case of DMMP are dissociated from the DFP and DMMP molecules to form methoxy and propoxy species on the surface when the samples are illuminated with solar light. The former species can be seen in the DMMP spectra in Fig. 6 at 1118 cm^{-1} in fair agreement with previous reports [18]. The pronounced peak

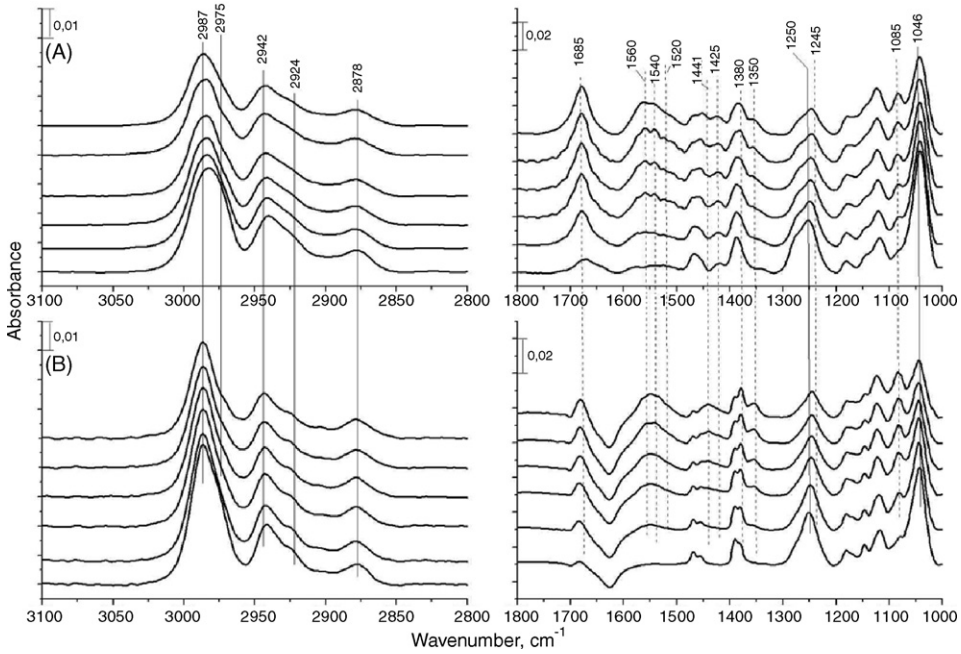

Fig. 5. Diffuse reflectance FTIR spectra of DFP adsorbed on rutile followed by 20 min of UV-irradiation of dry (A) and humidified (B) TiO_2, respectively. Each of the displayed spectra is separated by 4 min (top to bottom).

at 1685 cm^{-1} which appears after photooxidation of DFP can be assigned to the ν(C=O) mode in η^1-coordinated acetone, which is corroborated by the concomitant appearance of the ν(C–C) mode at 1245 cm^{-1}. The latter peak grows with increasing illumination time and complicates the analysis of ν(P=O) mode decomposition. This is also the reason for choosing the ν(C–O–(P)) in the quantitative analysis. The observation that acetone is one of the major surface intermediate in the photodegradation of DFP is not surprising, considering that the isopropyl groups are dissociated from DFP upon illumination. It is well known that photodegradation of isopropyl leads to acetone formation [3,16].

In contrast to DFP, acetone is not a major product of DMMP decomposition. It is known that the main product of photodegradation of methanol is formaldehyde in the aqueous phase [27,28]. In the gas–solid case surface bound methoxy species

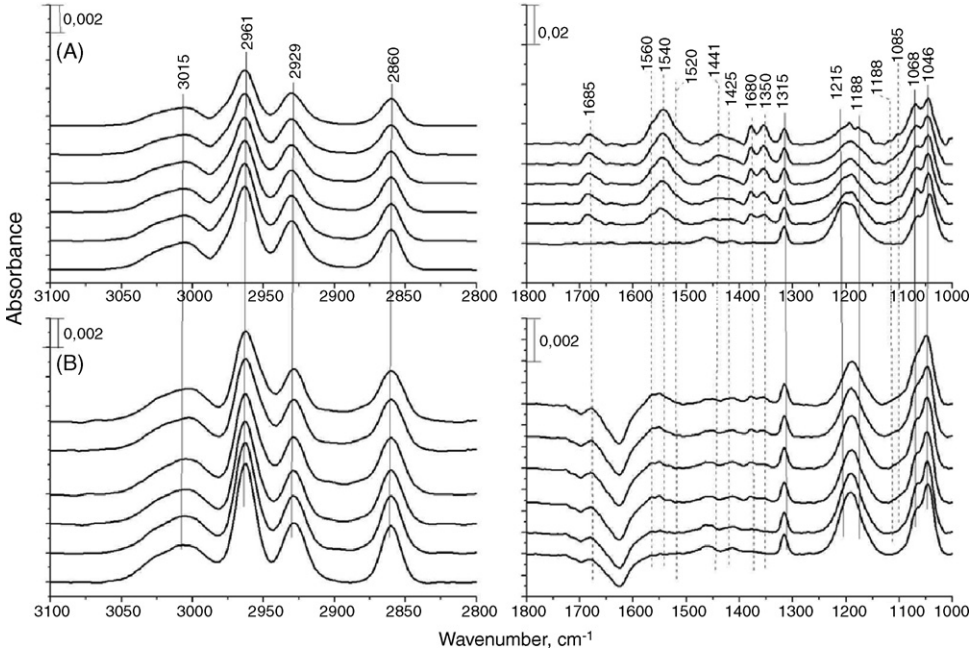

Fig. 6. Diffuse reflectance FTIR spectra of DMMP adsorbed on rutile followed by 20 min of UV-irradiation of dry (A) and humidified (B) TiO_2, respectively. Each of the displayed spectra is separated by 4 min (top to bottom).

form after reactions with surface OH and decompose to formic acid or surface bound formate [3,29], which further can transform to carbonate [30]. Interestingly, a peak still appears at 1685 cm^{-1} also in the case of DMMP photooxidation. Since this is not a photooxidation product, we tentatively attribute this to an aldol condensation-type reaction between, e.g. adsorbed DMMP and methoxy groups or carboxylate photooxidation products. This assignment is supported by the broadened higher energy shoulder of the 1215 cm^{-1} ν(P=O) peak indicating a weak ν(C–C) band. This is, however, a minority reaction as evidenced by the weak intensity of the 1685 cm^{-1} peak. Provided this interpretation is correct this also indicates that acetone formation may occur by at least two mechanisms also for DFP (and other organics). Aldol condensation mechanisms have previously been proposed also for the acetone/TiO_2 system [30].

It is difficult to discuss the changes that take place in the 1200–1300 cm^{-1} region in DMMP spectra because of the presence of two modes (ν(P=O) and ρ(P–CH_3)) in one wide band. Inspection of the δ(P–CH_3) vibrational loss at 1315 cm^{-1} shows that this bond is stable and is not destroyed during UV-illumination. This conclusion is in good agreement with previous reports [18]. Due to the stability of the P–CH_3 bond (Fig. 6), the transformation of the P=O group into a surface coordinated O–P–O group is slower for DMMP compared to DFP, which contains a F atom that is readily hydrolyzed as discussed above. Indeed, the decreasing intensity of the ν(P=O) mode at the 1250 cm^{-1} indicates that the fluorine atom is eliminated from the DFP molecule and that the P=O group is transformed into surface coordinated O–P–O species. This conclusion was proven by measuring of XPS spectra of rutile sample after 20 min of DFP dosing and after photocatalytic experiment (Fig. 7). Two lines of F 1s modes are observed in the spectra. The XPS peak with maximum at 689 eV should be assigned to fluorine bonded to an organic molecule (DFP) [31]. The second peak with maximum at 684 eV is typical for metal fluorides (titanium fluoride). It is seen that after photocatalytic experiment all fluorine atoms are dissociated from DFP and bonded to titanium as fluoride species. It is known from previous studies that F interacts strongly with the Ti cation, e.g. promoting crystallization in sol–gel synthesis [32] and giving rise to different branching of the reaction pathways in aqueous photocatalytic degradation of alcohols [33]. Incidentally, the former may partly explain the unusually large decrease of the BET area after photoreaction. The detailed structure of the O–P–O species that form when the P=O bond is cleaved is not known, but in analogy with previous studies [18,22], we attribute the peaks which develop in the 1100 cm^{-1} region in Figs. 5 and 6 to bridging bidentate O–P–O species.

Acetone, propoxy and methoxy groups are rapidly further decomposed and vibrational modes corresponding to coordinated formate-carboxylate-carbonate (R–COO^-) surface species dominate the DRIFT spectra after 20 min of solar light illumination. The absorption bands associated with these R–COO^- species occurs in the 1300–1600 cm^{-1} region for both DFP and DMMP. However, as discussed elsewhere, the discrimination of these species is non-trivial [12–15,34]. The asymmetric ν_{as}(OCO) modes overlap in the 1500–1580 cm^{-1} region, and the corresponding ν_s(OCO) modes overlap in the 1350–1400 cm^{-1}

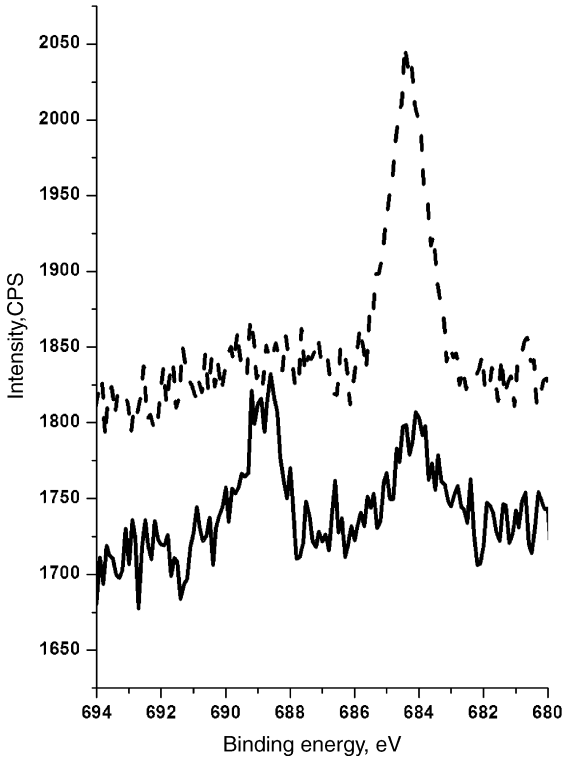

Fig. 7. F 1s XPS spectra of TiO_2 after 20 min of DFP dosing (solid line) and after 20 min of solar light illumination of the same DFP covered surface (dash line).

region where also the intense δ(C–H) mode in formate appears (~1370 cm^{-1}) [12–15,34]. The spectra in Figs. 5 and 6 agree, however, very well with a vibrational mode assignment, where bridge-bonded bidentate formate (μ-formate) at ~1540 and 1560 cm^{-1} (A and B types, respectively [35]), and bicarbonate at 1441 cm^{-1} [14,15,34] can be identified. The simultaneous evolution of absorption bands at 1560, 1380, and 2871 cm^{-1}, which may be attributed to the ν_{as}(OCO), δ(CH) and ν(CH) in bridge-bonded formate [13–15,34] provide further support that formate is a major intermediate after prolonged irradiation. Furthermore, the absorption band at 1520 and 1425 cm^{-1} can be assigned to acetate species [9]. In the 1100 cm^{-1} region surface coordinated O–P–O species appear (see above) and overlap with ν(CO) modes in Ti-bonded methoxy groups [17,26].

In Fig. 8 is shown the decay of the absorbance, A, of the ν(C–O–(P)) and δ(P–CH_3) bands, respectively, as a function of illumination time. The decay of the ν(C–O–(P)) band is well described by a first-order decay the first 20 min, viz. $\ln A = \ln A_0 - k_d t$, where A_0 is the absorbance at $t = 0$ and k_d is the degradation rate constants. It is evident from Fig. 8 that the rate of isopropyl dissociation is approximately 6–10 times faster for DFP than the corresponding methyl dissociation for DMMP. This shows further that the F abstraction destabilizes the adsorbed DFP molecule (see above). The rate of disappearance of the CH stretching modes is slower by a factor of 2–3 than the rate of isopropyl group dissociation for DFP. This shows that organic adsorbates accumulate on the surface (notably the R–COO^- species discussed above) and that the rate determining step for their total oxidation is the rate of R–COO^- oxidation. In

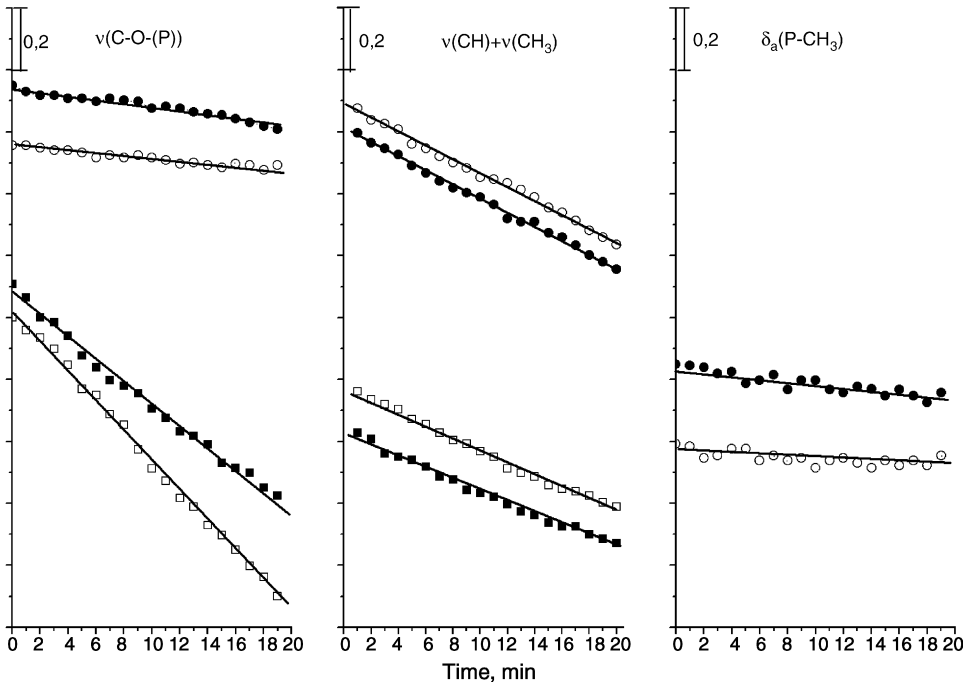

Fig. 8. The integrated intensity of the ν(C–O–(P)), δ(P–CH_3) and ν(C–H) absorption bands as a function of solar light illumination time on a dry (■) and wet (□) DFP preadsorbed rutile surface, and on a dry (●) and wet (◯) DMMP preadsorbed rutile surface.

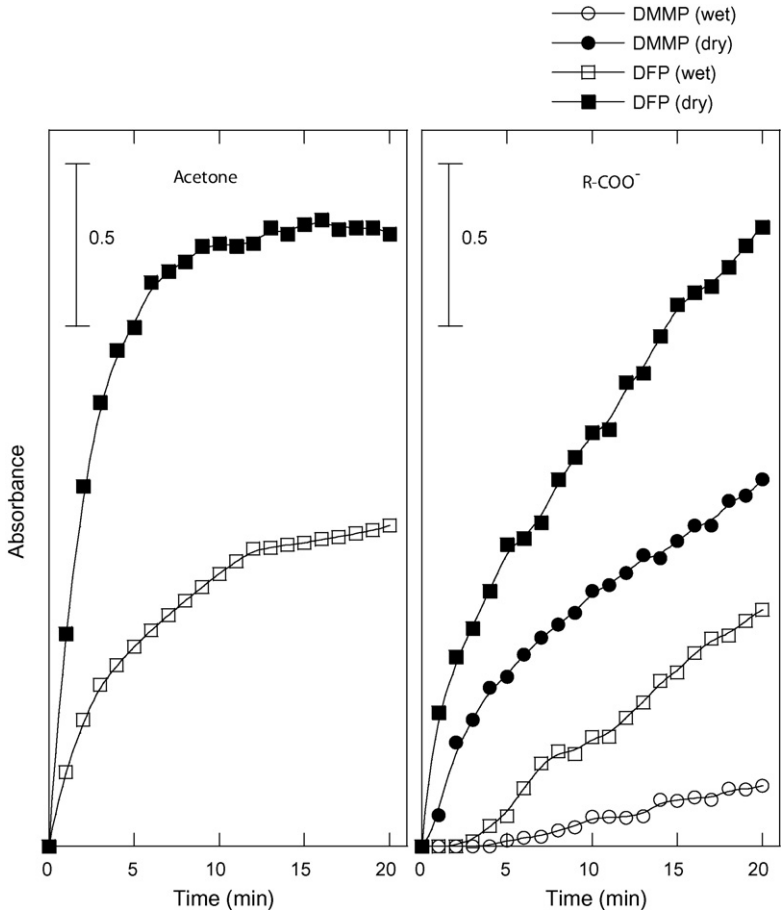

Fig. 9. The integrated intensity of the ν_a(OCO) modes due to adsorbed μ-coordinated R–COO^- species (1500–1600 cm^{-1}, region) and the ν(C═O) mode due to acetone (∼1685 cm^{-1}, peak) on a dry and wet rutile surface precovered with DFP (■ and □) and DMMP (● and ◯), respectively.

Table 3
Photodegradation rates, k_d, for isopropyl (*i*Pr), methyl (Me) and integrated C–H stretch region (2800–3100 cm^{-1}) in DFP and DMMP, respectively

Vibrational mode	k_d ($\times 10^{-4}$ s^{-1})			
	DFP		DMMP	
	Dry	Wet	Dry	Wet
ν(C–O–(P)) (*i*Pr or Me)	5.9 ± 0.1	8.1 ± 0.1	1.0 ± 0.3	0.7 ± 0.6
δ_s(P–CH_3) (Me)	–	–	0.9 ± 0.2	0.5 ± 0.25
ν(CH) + ν(CH_3)	3.1 ± 0.7	2.8 ± 0.9	2.9 ± 0.8	4.3 ± 1

contrast, for DMMP the rate of dissociation of the C–O–(P) and CH modes follows approximately the P–CH_3 dissociation rate (taking into account the different stoichiometry). This suggests that the rate determining step for DMMP photooxidation is the methyl bond dissociation. Finally, it is apparent from Fig. 8 that 2–3 ML water on the rutile surface gives no significant effect on either the DMMP or DFP photooxidation rate.

From Figs. 5 and 6 it is evident that the absorption bands due to R–COO– species are weaker on a wet surface than on a dry surface. We quantify this observation in the following. Fig. 9 shows the integrated intensity of the ν(C=O) acetone mode (1685 cm^{-1}) and the integrated asymmetric ν(OCO) bands due to R–COO– species (1500–1600 cm^{-1}) as obtained from the DFP spectra in Fig. 5 and the integrated asymmetric R–COO^- absorption band (1500–1600 cm^{-1}) from the DMMP spectra Fig. 6. In each case the data were normalized to integrated intensity of all $\nu(CH_3) + \nu$(CH) peaks apparent between 2800 and 3100 cm^{-1}, which were recorded after 20 min of DFP or DMMP dosing, respectively (Figs. 2 and 3). For both DFP and DMMP we find that the rates of acetone or carboxylate formation are higher on dry surface in comparison with humidified ones. Since it is reasonable to assume that there is initially approximately the same amount of DFP and DMMP, respectively, adsorbed on the dry and wet surface, the results in Fig. 9 together with those in Fig. 8 and Table 3 suggest that the surface coverage of intermediates (acetone and R–COO– species) is lower on the wet surface, and hence, that the total oxidation rate is faster in wet conditions, i.e. that key intermediates such as μ-formate are more easily decomposed on a wet surface. This can be rationalized if it is assumed that water blocks cation sites in the wet case (this is also seen in Figs. 2 and 3, where it was shown that hydrogen bonded rather than surface coordinated DFP and DMMP form upon adsorption) thus preventing formation of strongly bonded (bridging) formate-carbonate species on the surface. In the case of DFP where F bonds to Ti cations, it may be argued that the effect of water is superimposed on the changes induced by fluorination (e.g. suppression of surface OH hole trapping [33]). However, our similar results with DMMP do, however, shows that the effect that water has in preventing accumulation of strongly bonded formate-carbonate species, appears generally valid. Finally, we note that by increasing the water coverage on rutile, the DFP and DMMP decomposition rates decrease, which implies an optimum water coverage for sustained total oxidation [11].

4. Conclusions

Adsorption and photocatalytic degradation of DFP and DMMP over dry and humidified rutile prepared by hydrothermal treatment of microemulsions have been investigated. The isopropyl and methyl groups in DFP and DMMP, respectively, do not dissociate during adsorption on rutile, either on a dry or wet surface. The main initial products of DFP photooxidation are η^1-acetone and bridge-bonded (μ-coordinated) bidentate R–COO^- and P–COO^- species, while it is mainly μ-coordinated R–COO^- and P–COO^- species in the case of DMMP. In both cases μ-formate and P–COO^- species gradually accumulate on the surface. On a wet surface which contains only a few monolayers of water the concentration of intermediate surface species is reduced, while the rate of decomposition is approximately the same. The results show that it is possible to maintain a high photocatalytic degradation rate of organic phosphorous pollutants, while at the same time reducing unwanted accumulation of surface intermediates by adding a few monolayer of water on TiO_2. This implies a higher total oxidation rate by controlled humidification of the reaction gas. These results are in line with our previous findings for alkanes [11].

Acknowledgements

The work was funded through the Swedish Defense Nanotechnology Program (430-E46086) and the Swedish Ministry of Defense (430-A4515). A.E.C.P. thanks the Swedish Research Council for a senior researcher grant.

References

[1] O. Carp, C.L. Huisman, A. Reller, Prog. Solid State Chem. 32 (2004) 33.
[2] A. Mills, S. Le Hunte, J. Photochem. Photobiol. A 108 (1997) 1.
[3] J. Peral, X. Domenech, D.F. Ollis, J. Chem. Technol. Biotechnol. 70 (1997) 117.
[4] N. Serpone, A.V. Emeline, Int. J. Photoenergy 4 (2002) 91.
[5] A.J. Maira, K.L. Yeung, C.Y. Lee, P.L. Yue, C.K. Chan, J. Catal. 192 (2000) 185.
[6] V. Augugliaro, L. Palmisano, A. Sclafani, C. Minero, E. Pelizzetti, Toxicol. Environ. Chem. 16 (1988) 89.
[7] L. Cao, Z. Gao, S.L. Suib, T.N. Obee, S.O. Hay, J.D. Freihaut, J. Catal. 196 (2000) 253.
[8] S.B. Kim, S.C. Hong, Appl. Catal. B 35 (2002) 305.
[9] J.M. Coronado, S. Kataoka, I. Tejedo-Tejedor, M.A. Anderson, J. Catal. 219 (2003) 219.
[10] W.A. Jacoby, D.M. Blake, R.D. Noble, C.A. Koval, J. Catal. 157 (1995) 87.
[11] C. Hägglund, B. Kasemo, L. Österlund, J. Phys. Chem. B 109 (2005) 10886.
[12] F.P. Rotzinger, J.M. Kesselman-Truttman, S.J. Hug, V. Shklover, M. Grätzel, J. Phys. Chem. B 108 (2004) 5004.
[13] M. Andersson, A. Kiselev, L. Österlund, A.E.C. Palmqvist, J. Phys. Chem. B, submitted for publication.
[14] T. Lindgren, A. Mattsson, L. Österlund, J. Catal., submitted for publication.
[15] A.A. Davydov, Molecular Spectroscopy of Oxide Catalyst Surfaces, John Wiley & Sons, Chichester, 2003.
[16] A. Kiselev, M. Andersson, A. Mattsson, A. Shchukarev, S. Sjöberg, A. Palmqvist, L. Österlund, Surf. Sci. 584 (2005) 98.
[17] C. Rusu, J.T. Yates Jr., J. Phys. Chem. B 104 (2000) 12292.
[18] C. Rusu, J.T. Yates Jr., J. Phys. Chem. B 104 (2000) 12299.
[19] M. Andersson, L. Österlund, S. Ljungström, A. Palmqvist, J. Phys. Chem. B 106 (2001) 10674.

[20] M. Wu, J. Long, A. Huang, Y. Luo, S. Feng, R. Xu, Langmuir 15 (1999) 8822.
[21] A. Mattsson, M. Leideborg, K. Larsson, G. Westin, L. Österlund, J. Phys. Chem. B 110 (2006) 1210.
[22] A.E.T. Kuiper, J.J.G.M. van Bokhoven, J. Meema, J. Catal. 43 (1976) 154.
[23] G. Sokrates, Infrared Characteristic Group Frequencies, 2nd ed., John Wiley & Sons, Chichester, 1994.
[24] M. Primet, P. Pichat, M.-V. Mathieu, J. Phys. Chem. 75 (1971) 1216.
[25] R.I. Masel, Principles of Adsorption and Reaction on Solid Surfaces, 1st ed., John Wiley & Sons, New York, 1996.
[26] P.A. Connor, A.J. McQuillan, Langmuir 15 (1999) 2916.
[27] J. Marugan, D. Hufschmidt, M.-J. Lopez-Munoz, V. Selzer, D. Bahnemann, Appl. Catal. B 62 (2006) 201.
[28] L.Z. Sun, J.R. Bolton, J. Phys. Chem. 100 (1996) 4127.
[29] J. Araña, J.M. Doña-Rodríguez, C. Garriga i Cabo, O. Gonzãlez, J.A. Herrera-Melian, J. Pérez-Peña, Appl. Catal. B 53 (2004) 221.
[30] M. El-Maazawi, A.N. Finken, A.B. Nair, V.H. Grassian, J. Catal. 191 (2000) 138.
[31] J.F. Moulder, W.F. Stickle, P.E. Sobol, K.D. Bombem, in: J. Chastain, R. King Jr. (Eds.), Physical Electronics Inc., 1995.
[32] A. Hattori, M. Yamamoto, H. Tada, S. Ito, Chem. Lett. 27 (1998) 707.
[33] C. Minero, G. Mariella, V. Mauriono, D. Vione, E. Pelizetti, Langmuir 16 (2000) 8964.
[34] G. Busca, V. Lorenzelli, Mater. Chem. 7 (1982) 89.
[35] B.E. Hayden, A. King, M.A. Newton, J. Phys. Chem. B 103 (1999) 203.